Journal of Non-Crystalline Solids 550 (2020) 120359

Contents lists available at ScienceDirect

Journal of Non-Crystalline Solids

journal homepage: www.elsevier.com/locate/jnoncrysol

Effect of network formers and modifiers on the crystallization resistance of oxide glasses

Jeanini Jiusti[a], Edgar D. Zanotto[a,*], Steve A. Feller[b], Hayley J. Austin[b], Hanna M. Detar[b], Isabel Bishop[b], Danilo Manzani[c], Yuko Nakatsuka[d], Yasuhiro Watanabe[d], Hiroyuki Inoue[d]

[a] Graduate Program in Materials Science and Engineering, Federal University of São Carlos, São Carlos, Brazil
[b] Physics Department, Coe College, Cedar Rapids, United States
[c] São Carlos Institute of Chemistry, University of São Paulo, São Carlos, Brazil
[d] Institute of Industrial Science, The University of Tokyo, Tokyo, Japan

A B S T R A C T

In this work we used two glass stability (GS) parameters, which best correlate with the glass-forming ability (GFA), in an extensive study for analyzing the influence of alkali and alkaline earth modifiers and five glass-formers, in the crystallization resistance of binary oxide glasses. For the good glass formers silica, boria and germania, the addition of small amounts of *modifiers* rapidly reduces the GS, whereas for the conditional glass formers telluria and alumina, it initially increases the GS. Lower liquidus temperatures are associated with a better GS, and above 50 molar percent of modifier oxide, the liquidus temperature seems to be the main factor controlling GS (except for telluria). Lithium containing glasses show the lowest GS between the alkali systems, while the alkaline earth modifiers show the same effect on the GS. The TeO_2 is the only exception, for which the barium tellurites show better GS. The pure oxides rank in the following order of GS: $B_2O_3 > SiO_2 > GeO_2 > TeO_2 > Al_2O_3$.

1. Introduction

Due to their absence of microstructure (for compositions that are free of liquid phase separation) and smooth property-composition dependence, glasses can show unique, adjustable properties, such as low, moderate or high transparency in the UV, visible or IR, bioactivity, ionic conductivity, hardness, elastic modulus, refractive index, thermal expansion coefficient, chemical durability, etc.

The addition of network modifiers to pure oxide glass-formers, such as SiO_2, B_2O_3, GeO_2, Al_2O_3 and TeO_2, induces changes in the glass structure and significantly modify certain properties. Understanding the individual effect of the glass network modifiers – alkali and alkaline-earth cations (Li, Na, K, Rb, Cs, Mg, Ca, Sr and Ba) – is important to aid and shorten the design of new compositions. For instance, the effect of alkali and alkaline earth oxides on the thermal expansion coefficient, glass transition temperature, refractive index, density, elastic modulus and other intensive properties of binary glass-forming systems has been widely studied, especially for silicates and borates [1–9]. It is known, for example, that the thermal expansion coefficient (α) of alkali and alkaline earth borates and silicates increases with the modifier cation radius [6,10]. Similar behaviors have also been observed for other properties [11]. Despite the great effort and progress on understanding the effect of those simple modifiers on several glass properties, the relationship between the amount and type of each **modifier** and the **glass resistance to crystallization** has been much less explored.

The resistance that certain glass-forming substances show against crystallization is one of its most important properties, because it limits the size of the glass piece that can be obtained, and consequently, its manufacturing process and final application. When analyzed on the cooling path of a melt from the liquidus temperature, the resistance against crystallization is called “glass-forming ability” (GFA), and when it is analyzed on the heating path of a glass above T_g, we call it “glass stability” (GS). The GFA and GS depend upon the material´s composition, which in turn control the crystal nucleation and growth rates. These have been studied elsewhere [12–16].

The determination of GFA is very time-consuming by conventional methods, such as the time-temperature-transformation (TTT) curve [17], the thermocouple method [18] or the Colmenero and Barandiarán method [19]. To avoid this problem, many simple parameters based on the characteristic temperatures of glasses and supercooled liquids have been suggested [12,14,20–42] to estimate GFA. These parameters are calculated using the characteristic temperatures determined by differential thermal analysis (DTA) or differential scanning calorimetry (DSC): the glass transition temperature (T_g), the onset of crystallization (T_x), the crystallization peak (T_c), and the liquidus temperature (T_l). Because these temperatures are often determined during the *heating* of a

* Corresponding Authors.
E-mail addresses: Jeaninijiusti@gmail.com (J. Jiusti), dedz@ufscar.br (E.D. Zanotto).

https://doi.org/10.1016/j.jnoncrysol.2020.120359
Received 30 June 2020; Received in revised form 27 July 2020; Accepted 8 August 2020
Available online 05 October 2020

Table 1
GS and GFA classification according to the ΔT_{rg} and K_H parameters: powdered samples (< 60 μm) using T_x and heating rate of 10–20 K/min.

GS and GFA	ΔT_{rg}	K_H	Maximum glass sample thickness
Outstanding	> 0.6	> 1.1	m
Good	0.4–0.6	0.7–1.1	several cm
Reluctant to Poor	0.1–0.4	0.2–0.7	mm - cm
Extremely Poor	< 0.1	< 0.2	μm - mm

glass sample, we call them "glass stability" parameters.

Among the approximately 30 parameters proposed in the literature, the Hrübý number $K_H = [(T_x-T_g)/(T_l-T_x)]$, has been proved to be a good estimator of the GFA by several authors [15,21,43–45]. Moreover, recently, a similar parameter, $\Delta T_{rg} = [(T_x-T_g)/(T_l-T_g)]$ [30], that has the advantage that it varies from 0 to 1, has been pointed out as another good estimator of GFA. Both GS parameters show a good linear correlation with the critical cooling rate ($R_c = 1/GFA$) for glass formation, and also have an ability to predict with good statistical accuracy the R_c, as demonstrated in a previous paper [16]. Therefore, they are appropriate metrics to discover the effect of alkali modifiers on the resistance against crystallization (both GS and GFA) of different glass-forming systems.

Table 1 summarizes the GS / GFA and some approximate numbers used to distinguish the vitrification ability of different liquids. This classification was created based in our previous publications [16,46] and experimental knowledge acquired in over 40 years of laboratory glass-making, which includes this work. For instance, typical commercial bulk glasses, made by traditional glass forming techniques, have values of GS above 0.4 (ΔT_{rg}) and 0.7 (K_H). Hence, this table gives the overall "ball park" of widely distinct GS and GFA, and serves as a guide to understanding the next plots describing the GS versus chemical compositions. An estimate of the maximum glass sample thickness for each class is informed in the last column.

The aim of this work is to understand the **effect of alkali and alkaline earth modifiers on the resistance against crystallization of five glass-formers**: SiO_2, B_2O_3, GeO_2, TeO_2 and Al_2O_3. The results may help to design better glass compositions and also to comprehend the key factors involved in the GS and GFA. For this task, we collected characteristic DSC temperature data for many binary oxide glasses (modifier + glass former), and briefly discussed the effect of the modifiers on the structure of these binary glasses to explain their GS behavior by using the K_H and ΔT_{rg} parameters, which allow us to compare their thermal stability in a quantitative way.

2. Experimental

2.1. Sample preparation

The binary glass compositions were prepared in the form of xR_2O-$(100-x)F_yO_z$ and xRO-$(100-x)F_yO_z$, where R_2O is the alkali oxide (Li_2O, Na_2O, K_2O, Rb_2O and Cs_2O), RO the alkaline-earth oxide (MgO, CaO, SrO and BaO), F_yO_z is the glass-former oxide (SiO_2, B_2O_3, GeO_2, TeO_2 and Al_2O_3) and x is the molar percent of network modifier oxides. The preparation procedure of all glasses is detailed below. All precursor powders were dried in a drying oven at 100 °C for at least 24 h before use.

The silicates and germanates studied in this work were produced in the Laboratory of Vitreous Materials (LaMaV), Brazil, by the conventional melt-quenching technique. The precursor powders SiO_2 (Zetasil, 99.99%), GeO_2 (Alfa Aesar, 99.99%), Li_2CO_3 (Sigma Aldrich, 99.0%), Na_2CO_3 (Sigma Aldrich, 99.5%), K_2CO_3 (Sigma Aldrich, 99.5%), Rb_2CO_3 (Sigma Aldrich, 99.0%), Cs_2CO_3 (Alfa Aesar, 99.0%), MgO (Sigma Aldrich, 99%), $CaCO_3$ (JT Baker, 99%), $SrCO_3$ (Alfa Aesar, 99%) and $BaCO_3$ (Sigma Aldrich, 99.0%) were mixed in a translational mixer for 4 h. The compositions were melted at ~50 °C above the respective liquidus temperatures in Pt crucibles for one hour, homogenized and quenched in stainless steel plates (splat cooled).

The alkali borate glasses were produced via carbonate method (CM) [46] at Coe College, USA. Alkali carbonates (Li_2CO_3, Na_2CO_3, K_2CO_3, all Sigma Aldrich, > 99%), and boric acid (H_3BO_3, Sigma Aldrich, > 99%), powders were mixed together thoroughly and heated at 1000 °C for 25 min in a platinum crucible. A weight loss check was made in-between of heating to confirm the sample composition and the sodium borate glasses showed some carbonate retention at alkali content exceeding about 66 molar percent alkali oxide. Then, the lithium borate melts were either plate or twin-roller quenched in room environment conditions [47]. After the weight loss check, the sodium and potassium borates were heated and roller-quenched inside a glove box, a nitrogen gas and a low water environment. The $BaO{\bullet}2B_2O_3$ and $SrO{\bullet}2B_2O_3$ glasses ($SrCO_3$ and $BaCO_3$ 99.9%, and H_3BO_3 99.5%, all Wako Chemicals) were produced in The University of Tokyo, Japan. They were melted in lidded platinum crucibles, 80 °C above their respective melting point, for 30 min, and then they were splat cooled.

Alkali and alkaline earth tellurite glass samples containing 5 and 15 molar percent of modifier oxide were also prepared by melt-quenching in the University of São Paulo, Brazil. The chemicals TeO_2 (Prichem, 99.99%), Li_2CO_3 (Sigma Aldrich, 99%), Na_2CO_3 (Sigma Aldrich, > 99%), K_2CO_3 (Merck, 99%), Rb_2CO_3 (Sigma Aldrich, 99%), Cs_2CO_3 (Sigma Aldrich, 99%), $CaCO_3$ (Merck, 99%), $SrCO_3$ (Sigma Aldrich, 98%) e $BaCO_3$ (Alfa Aesar, 99%) were stoichiometrically weighed to obtain 3 g of glass, thoroughly mixed in a translational mixer, and then loaded into a Pt/Au alloy lidded crucible. The samples were melted at 700 to 900 °C, for 20 min in a muffle furnace. The glass melts were cast into stainless steel plates or in cold water (see Table S1.1 in supplementary materials).

The aluminate glasses were prepared using an Aerodynamic Levitation (ADL) furnace [48] at The University of Tokyo, Japan. Alkaline earth oxides (MgO 99.9%, CaO 99.5%, SrO 99.9% and BaO 99.9%, Wako Chemicals) and Al_2O_3 (High Purity Chemicals, 99.99%) powders were mixed in acetone and pressed into 2 g tablets, which were sintered for 12 h at 1100 °C in air and crushed into 20–50 mg fragments. The fragments were levitated by a flow of N_2 and melted using a 100 W CO_2 laser to around 2300 °C. Then the melt was rapidly cooled by shutting off the laser power at a cooling rate of approximately 800 °C/s. The final samples were small spheres of ~ 2 mm diameter.

The chemical compositions of the glass samples were checked using a Jeol JSX-3100RII X-ray Fluorescence Spectrometer. Only the borate compositions were not measured due to the low boron atomic weight. The measured composition of glasses deviated about 1–2% (mol content) of the nominal composition.

2.3. Thermal analysis and data collection

The characteristic temperatures T_g, T_x, and T_c were experimentally determined for the glasses prepared in this work using a Netzsch DSC 404 at the Federal University of São Carlos, Brazil and a TA DSC Q200 or Perkin-Elmer DSC 7 at Coe College, USA. To complement the analysis, the characteristic temperatures of other binary glass compositions of the systems studied were collected from the SciGlass® v. 4.11 database. All data collected from the literature and measured in this study were determined in similar conditions; fine powders (< 100 μm in size) and heating at 10–20 K/min in atmospheric air. Using fine powder privileges heterogeneous nucleation, therefore reducing the effect of internal nucleation (shown by a few compositions). The T_l were collected from the respective phase equilibrium diagrams. The collected and measured data are shown in section S1 of the supplementary materials.

3. Results and discussion

The goal of this study was to determine the effect of the most common network *modifiers* (alkali and alkali earth) and network *formers* (Si, B, Ge, Te, and Al) on the resistance of oxide glasses against crystallization. As previous works have shown [15,36,43–45], the two GS parameters used in this study correlate quite well with the glass-forming ability of oxide glasses, hence, their GFA will also be discussed. The results will be presented and discussed separately for each group.

Before we present the results, we introduce here our strategy to qualitatively explain GS-composition trends. As GS is a measure of the glass resistance against crystallization upon **heating**, some key aspects involved in nucleation, crystal growth and overall crystallization can be used to explain the behavior of the systems studied. To this end, the most important variable controlling crystal nucleation is the interfacial energy (σ) between the crystalline nuclei and the supercooled liquid (SCL) [49,50], then comes the thermodynamic driving force (ΔG), and the diffusivity (D). Once a critical nucleus forms, crystal growth is a spontaneous process without any thermodynamic barrier; only the kinetic barrier remains. Therefore, diffusivity is the main controlling parameter of this process. Also, as in a wide temperature interval ($1.15\ T_g - T_l$), the Stokes-Einstein theory is valid, the effective diffusion rates controlling crystal growth are inversely proportional to the viscosity. Therefore, because *σ* relates to the difference between the structures of the SCL and the nucleated crystal (the smaller the structural differences, the smaller σ and higher nucleation rates) [51] and the *viscosity* is strongly determined by the glass network connectivity and chemical bonding, glass structure is a key parameter to understand GS. Hence, in the following sections, we will use these concepts to some extent in an attempt to (qualitatively) explain the observed trends of GS / GFA with the chemical composition of the glasses.

3.1. Effects of alkalis and alkaline-earths

3.1.1. Silicate glasses

The two GS parameters of alkali and alkaline earth silicates are shown in Fig. 1. The ΔT_{rg} of silica (SiO_2) glass is considered = 1 because no crystallization peak was detected during our thermal analysis experiments. Silica glass is quite stable against crystallization and easily vitrifies when cooled from the liquid state. Some authors have estimated a very small critical cooling rate of $\sim 10^{-6}$ K/s [52,53] for this substance. Structurally, this great stability can be related to the high degree of connectivity of the tetrahedral SiO_4 units (Q^4, 4 stands for four bridging oxygens per tetrahedron) in the random network [54].

It should be stressed that addition of alkalis and alkaline earth oxides to silica leads to regions of stable or metastable liquid phase separation (LPS). In the *alkali* silicate systems, the metastable (sub-liquidus) miscibility gaps extend up to approximately 31 molar percent of Li_2O and 23 of Na_2O [55]. In Fig. 1 only four data points of the lithia-silica system are within the miscibility gap, and indeed the samples we made in this composition range were translucent. On the other hand, LPS is absent in all alkali-rich compositions of the Na_2O-SiO_2 and K_2O-SiO_2 systems studied here.

In the case of the *alkaline earth* silicate systems, the MgO-SiO_2, CaO-SiO_2 and SrO-SiO_2 show stable (above the liquidus) liquid miscibility gaps, which extend up to approximately 40, 30 and 20 molar percent of RO, respectively [56]. Therefore, we collected data for compositions outside these immiscibility regions. In the Ba-silicate system, there is a metastable miscibility gap extending up to ~29 molar percent of BaO [55].

Fig. 1 shows that as the amount of alkali increases, the GS decreases. Among the *alkali* silicates, the lithium silicate glasses are by far the most prone to crystallize, showing ΔT_{rg} and K_H parameters in the 0.15 - 0.20 range up to 40 molar percent of Li_2O, when they decrease dramatically leading to what is popularly known as the “limit” of glass formation (using standard laboratory practices). Fig. 1 shows a strong decrease in both GS metrics for small amounts of Li, in the immiscibility range, and then a shallow maximum at around 30 molar percent of Li_2O, which is close to the eutectic region of the phase equilibrium diagram. In fact, it is (empirically) known that compositions close to deep eutectics tend to have good glass-forming ability and stability [30].

The sodium silicates showed much higher GS than the lithium silicates, and the maximum was, once more, near the eutectic region (~30 molar percent of Na_2O). For the potassium silicates, however, there are not enough data points to conclude whether the highest GS is located close to the first eutectic (~20 molar percent of K_2O), but the ΔT_{rg} parameter is indeed higher for 20 than for 33 molar percent of K_2O. We also made Rb and Cs silicate glasses, but they were extremely hygroscopic. Hence, we could not measure their characteristic DSC temperatures to calculate the respective GS parameters. Therefore, we conclude that as the cation radius increases, the glass stability increases in the following sequence: K > Na > Li-silicates. However, the high thermal stability of the Na and K glasses, comes with a substantial decrease of the chemical stability, which become more hygroscopic in the same sequence, including the Rb and Cs glasses, which are so hygroscopic that the measurements were not feasible and the analysis of GS was not possible.

The addition of alkali modifiers to silica results in a substantial decrease of the glass stability due to the reduction in the network connectivity by creation of non-bridging oxygens (NBO). For each R^+ added to the glass network, one NBO is formed per SiO_4 tetrahedra, resulting in Q^3, Q^2, Q^1 and even Q^0 units. At low R_2O concentrations, up to 33 molar percent of R_2O, most Q^4 units are replaced by Q^3 and Q^2 units. Further addition of R_2O leads to transformation of some Q^3 to Q^2 and Q^1 units, with increasing amount of non-bridging oxygens as the content of R_2O increases. The observed concentration of Q^n units are qualitatively explainable according to disproportionation reactions: $2Q^3 \rightarrow Q^4 + Q^2$; $2Q^2 \rightarrow Q^3 + Q^1$ and $2Q^1 \rightarrow Q^2 + Q^0$ [57]. In general, the reduced network connectivity facilitates the structural rearrangements needed for crystallization, and therefore, the GS is reduced.

The structures of Li, Na, K, Rb and Cs silicate glasses are very similar, with some changes in the disproportionation reactions, which tend to the left (higher n) for larger cations [58,59]. By comparing their structures with their isochemical crystals, we can find some answers. After analyzing the structures of Li and Na disilicates, Longstaffe et al. [60] observed that while the lithium disilicate glass has an intermediate-range structure very similar to its isochemical crystal, the sodium disilicate system shows significant differences. The strong similarity between the intermediate range structure of $Li_2O.2SiO_2$ crystal and glass explains why this alkali disilicate displays measurable homogeneous nucleation rates, while the others do not show internal nucleation [60]. However, this would not be an important effect for our study because we used powdered samples in the DSC experiments and the internal nucleation rates are relatively small in Li silicates compared to the surface density of sites in powdered samples.

In powdered samples, copious heterogeneous surface nucleation predominates, hence crystallization differences of distinct compositions are mainly controlled by differences in their crystal growth rates (U). Considering the available crystal growth models, and that the mechanism controlling diffusion is the same that control viscous flow (Stokes-Einstein Eyring) [61,62], one can conclude that U is proportional to the relation T_l/η (η = viscosity) [53]. As the viscosity is a function of network connectivity, it is expected that formation of NBO's diminishes the viscosity. In fact, the viscosity of silica (SiO_2) at 1600 K, for example, is nine orders of magnitude greater than those of the Li, Na and K disilicate melts at the same temperature. Near T_g, diffusion of structural units controlling crystal growth is decoupled from viscosity, and the diffusion of smaller species, like Li can be favored. This can be one of the reasons for the Li silicates showing lower GS.

Above 50 molar percent of R_2O, the network connectivity is already very low, and the viscosity is expected to show negligible change with composition; hence the liquidus temperature itself plays a more

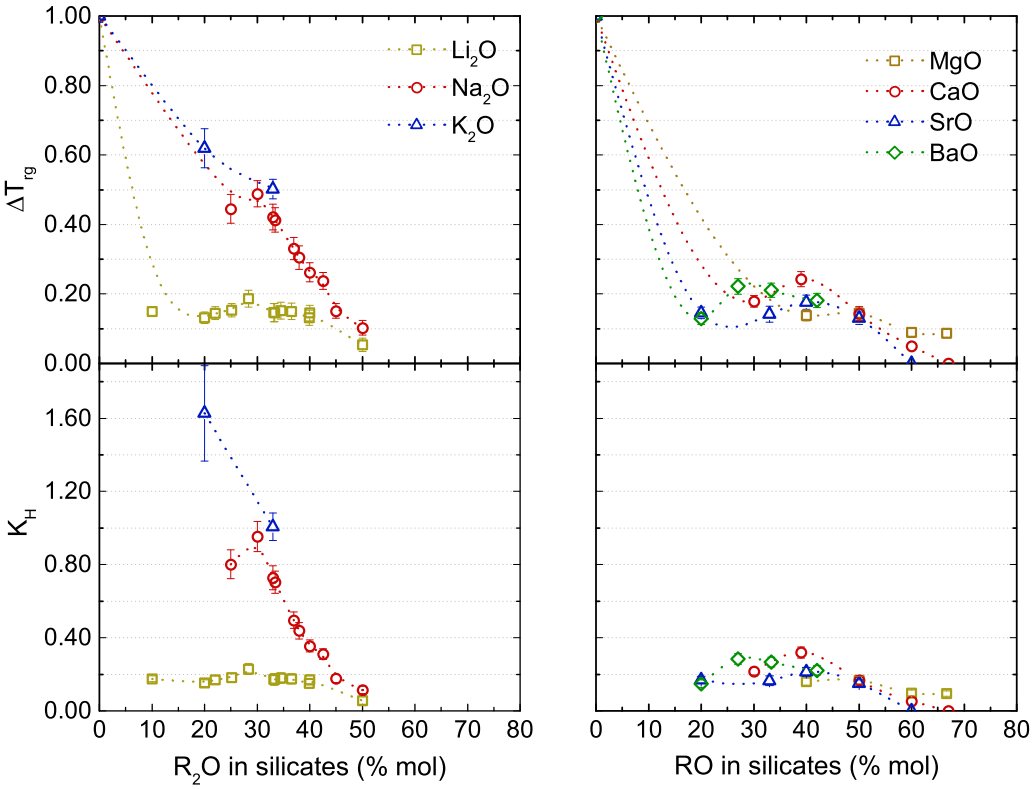

Fig. 1. Glass stability parameters, ΔT_{rg} and K_H, for a series of binary alkali (left) and alkaline earth (right) silicate glasses. Powdered samples (particle size < 100 μm), heating rate = 10 to 20 K/minute.

important role. Although the temperature dependence of viscosity is similar for all the alkali silicates, the liquidus temperature of the lithium silicates are notably higher (Figure S2.1 in the supplementary materials). As both GS parameters used here are inversely proportional to the liquidus temperature, T_l, any glass with higher T_l (and similar T_g and T_x) will have a lower GS and GFA, which is indeed a relation empirically observed in laboratory practice.

The plot on the right-hand side of Fig. 1 shows the GS parameters for the *alkaline earth* silicates. Glasses with RO molar content above 50% were obtained by ADL, and the rest was obtained by splat cooling. Due to the high volatility of BaO, we could not obtain barium silicates using the ADL furnace, thus, only silicates with BaO content below 50% were studied. For all these alkaline earth network modifiers, we see a sharp decrease of GS down to a region of very low glass stability (ΔT_{rg} = 0.1–0.2 and K_H < 0.3), indicating that Mg, Ca, Sr and Ba have approximately the same effect on the GS of silicates. We decided not to test Be because it is too poisonous.

Although a mole of RO (R^{2+}) introduces the same amount of NBO as a mole of R_2O ($2R^+$), the reduction in GS and GFA occurs more abruptly in the alkaline earth silicates than in the Na and K silicates. This result can be explained by the higher liquidus of the alkaline earth silicates, which are even higher than the liquidus temperatures of the Li_2O-SiO_2 system. In fact, Li and alkaline earth silicates have a similar behavior. The glass-forming region extends to a higher content of MgO, because of the lower liquidus of this system in the network modifier-rich region. (All characteristic temperatures of the silicate glasses are shown in Fig. S2.1 in the supplementary material).

3.1.2. Borate glasses

The ΔT_{rg} and K_H parameters of borate glasses are shown in Fig. 2. Thermal analyses of pure B_2O_3 did not reveal any crystallization peak; therefore, for practical purposes, we assigned an arbitrarily high value of ΔT_{rg} = 1. This glass is known to have exceptional glass stability, and, to best of our knowledge, the crystallization of B_2O_3 glass at ambient pressure has never been reported. The reason for this outstanding GS was fully discussed by Zanotto and Cassar [63].

The alkali-borate systems also show sub-liquidus (metastable) miscibility gaps, approximately between 2 and 20 molar percent of Li_2O, 8–24 molar percent of Na_2O and 2–22 molar percent of K_2O [64]. The GS trend observed in Fig. 2 seems to be smooth and not affected by immiscibility. The Li-borates are somewhat below the other two but, in general, these three alkali modifiers affect the GS of borates in a similar way, with almost no difference between the GS values. However, there are some exceptions, e.g. for the Li, Na, and K diborates, we observe that lithium diborate has the poorest GS, followed by the potassium and sodium diborates ($GS_{Li} < GS_K < GS_{Na}$). This is the same relation observed for the liquidus of this particular R_2O content in borates. And, as for the silicates, Li-borates are the only to show internal (homogeneous) nucleation, in addition to surface crystallization. The GS reaches a minimum value at 50 molar percent of R_2O, and remains constant up to the end of the glass-forming region.

The ΔT_{rg} and K_H parameters for alkaline earth borates are shown in Fig. 2 (right hand side). The region of liquid immiscibility is located in the B_2O_3 rich area, and reaches up to 33% MgO, 30% CaO, 20% SrO and 15% BaO, approximately [65–68]. The greater glass-forming region occurs for barium borates, followed by strontium, calcium and magnesium borates, the last having a glass-forming region very narrow, from 45 to 55 molar percent of RO [7]. Because the glass-forming region of the MgO-B_2O_3 system is very narrow, there is no information about the characteristic DSC temperatures, hence the GS metrics could not be calculated for this particular system.

As observed for the R_2O, the GS of borate glasses also decreases in a nearly monotonic trend with the RO content in the range studied, with no statistical difference between these network modifiers. The ΔT_{rg} decreases in a very similar ratio as for the alkali borates, reaching values below 0.20 for RO > 30. At the eutectic composition, near to 60% BaO, there is a small increase in GS for the reasons already mentioned.

Regarding the structural aspects, pure vitreous B_2O_3 is composed of

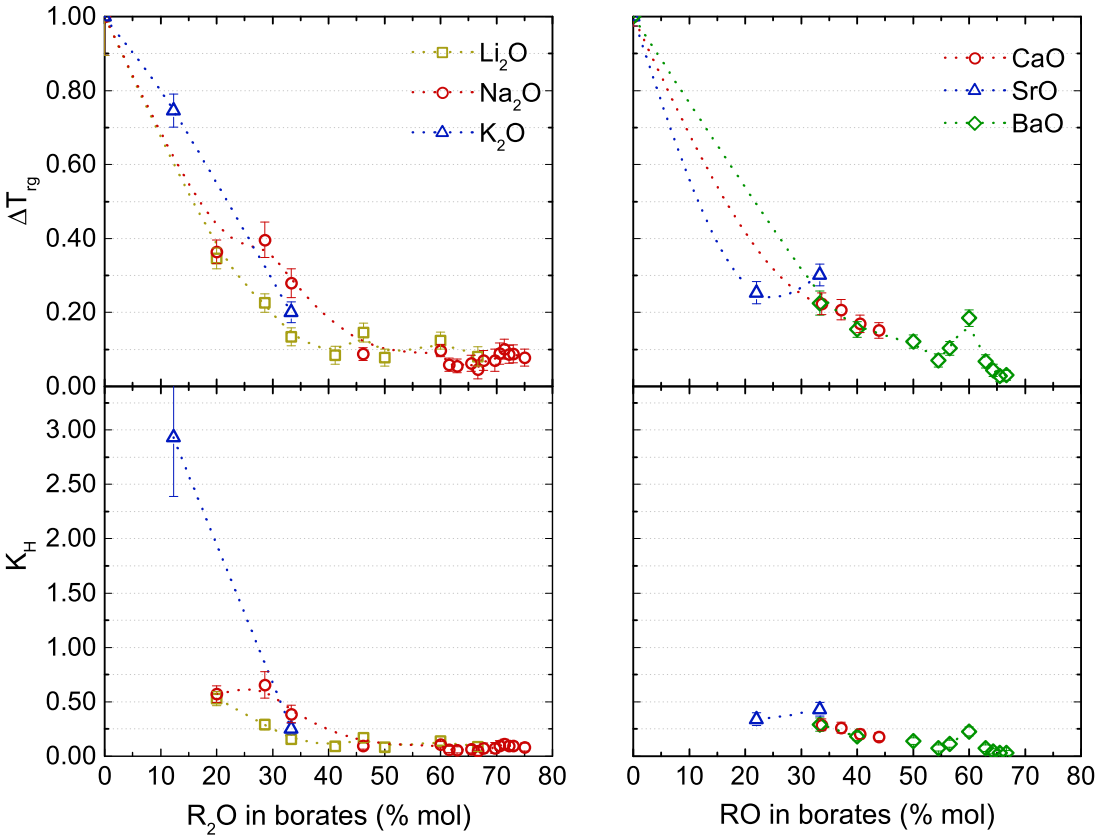

Fig. 2. Glass stability parameters ΔT_{rg} and K_H for a series of binary alkali (left) and alkaline earth (right) borate glasses. Powdered samples (particle size < 100 μm), heating rate = 10 K/minute.

triangular BO_3 units which combine into boroxol rings (70% of the B atoms), and the addition of modifier oxides results in the creation of BO_4 units up to ~35 molar percent of R_2O and RO (the exact amount depends upon the cation), without significant formation of non-bridging oxygens [69]. At higher network modifier content, the proportion of BO_4 units decreases and the number of NBOs increases, leading to the depolymerization of the glass network. The overall result is a maxima of BO_4 units around ~35 molar percent of R_2O, called the "borate anomaly", and it is also observed in other properties like T_g, density and thermal expansion coefficient [1,6]. The borate anomaly, however, occurs simultaneously with an increase of the *liquidus* temperature, and the overall result is a continuous decline of ΔT_{rg} and K_H. For comparison we can take the ΔT_{rg} of lithium diborate, 0.13, which has a very low glass stability and is very difficult to vitrify. Above ~40 molar percent of R_2O, the ΔT_{rg} parameter becomes even smaller, and glasses can only be obtained by non-conventional methods, e.g., by the twin roller quenching method used in this work.

3.1.3. Germanate glasses

The glass stability parameters of several binary alkali and alkaline earth germanate glasses are shown in Fig. 3. Pure GeO_2 glass has a very good glass stability (K_H~1.3), but it is less stable than SiO_2 and B_2O_3. As in silica, the structure of GeO_2 is formed by a continuous random network of corner sharing tetrahedra, but a greater distortion of the tetrahedra is observed, and the rings are composed by smaller numbers of tetrahedral units [70,71]. This structural difference accounts for an easier conversion to crystals [70]. Additionally, GeO_2 has a lower viscosity than SiO_2 glass, which fosters faster diffusion and, therefore, leads to a lower GS. GeO_2 shows an estimated critical cooling rate of approximately 10^{-3} K/s [13,36,52,53,72,73], two orders of magnitude higher than that of silica glass (this value is only an approximation that depends on the assumptions considered in the calculations).

The alkaline earth germanate systems also present stable and metastable immiscibility regions. Tabata et al. [74] determined that the miscibility gaps extend to 30% MgO, 24% CaO, 16% SrO and 10% BaO. Therefore, immiscibility in the high alkali-GeO_2 regions studied is unlikely [75].

As observed for the silicates, additions of alkali and alkaline earth modifiers decrease the glass stability, however we observe a minimum GS at around 20 molar percent of modifier oxide. This behavior mimics the effect of the alkali modifiers in the molar volume of germania, reported by Shelby [5,76].

Although there are contradictions in the literature [77,78], one view is that the addition of alkali oxides to GeO_2 leads to an increase of the average Ge coordination number, as the main mechanism to incorporate the oxygen surplus, instead of straightforward creation of NBO's. This unusual structural change reflects in the glass stability, as well in other properties, as an anomaly, showing a minimum or maximum at around 20 molar percent of R_2O and RO. In the case of the GS, we see a minimum, at least for the Li_2O, Na_2O, K_2O, SrO, CaO and BaO, modified germanates, for which we have enough data. This happens due to the proneness of the higher coordinated Ge atoms containing glass towards crystallization. Further addition of R_2O and RO will lead to the creation of NBO's, and the average coordination of Ge starts to decrease again, reducing the propensity to devitrification. The GS is expected to decrease again at some point, because the excessive amount of NBO's, but we do not have data for compositions with more than 40% modifier oxides. Unfortunately, there are no published viscosity data for these germanates.

As seen for the SiO_2 systems, the effect of lithium in decreasing the GS is more accentuated than that of the other modifiers, thus, for germanate glasses: $GS_{Li} < GS_{Na} < GS_K < GS_{Rb} < GS_{Cs}$. We also observed this trend in our own laboratory experiments; the Li_2O-GeO_2 system shows the highest liquidus temperature, which can justify this behavior. In

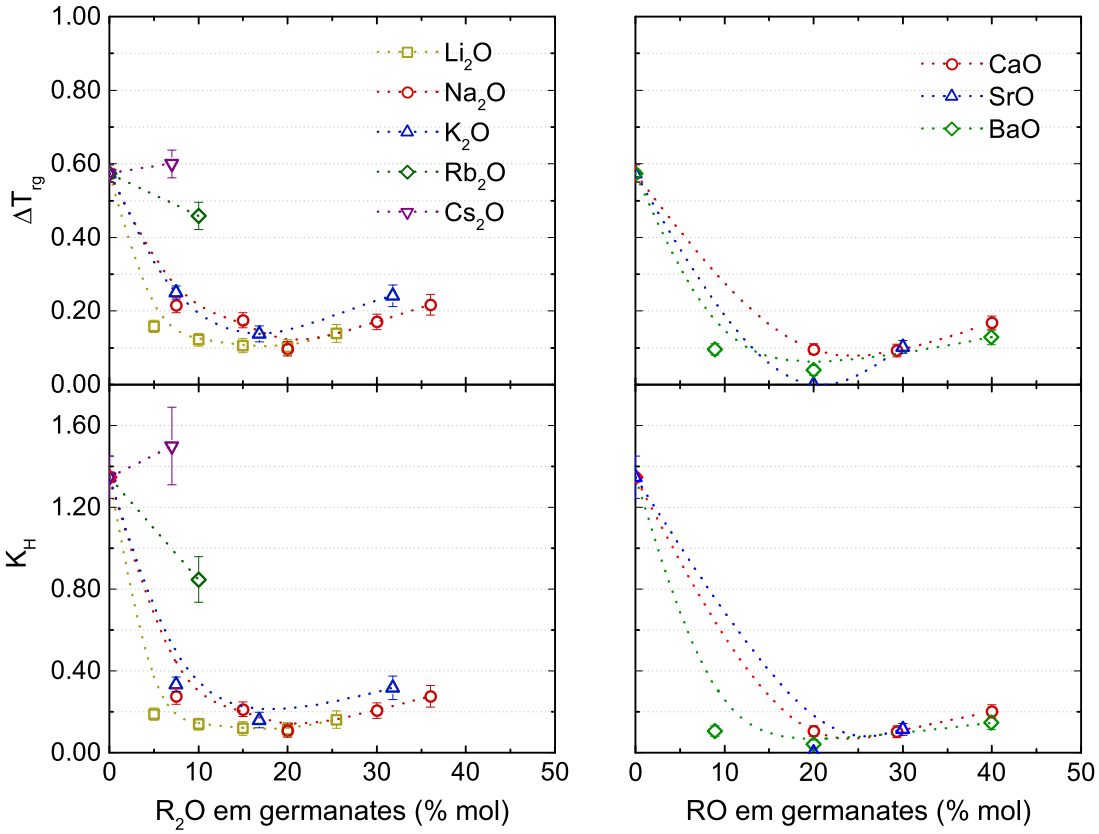

Fig. 3. Glass stability parameters, ΔT_{rg} and K_H, for a series of binary alkali (left) and alkaline earth (right) germanate glasses. Powdered samples (particle size < 100°μm), heating rate = 20 K/minute.

addition, the germanates are more difficult to vitrify than the borates and silicates. There is no clear distinction between the effect of the different alkaline earth elements, however these results show that the glass stabilities of the RO germanates are lower than those of the R_2O germanates.

3.1.4. Tellurite glasses

Fig. 4 shows the ΔT_{rg} and K_H parameters for several tellurite glasses. Differently from the other three glass forming systems studied, pure TeO_2 is a very reluctant glass former and must be obtained by non-usual methods, for example using a twin-roller quencher [79], which reaches a cooling rate of 10^5 K/s [47], or by quenching the crucible bottom into a liquid at low temperature [80]. Corroborating these experimental observations, Fig. 4 shows that pure TeO_2 has a very small ΔT_{rg}, and, indeed, from DSC traces (not shown), we observed that the crystallization peak starts right after the glass transition. The structure of pure TeO_2 is still under discussion, but is believed that TeO_2 glass is mainly composed by trigonal bipyramids (tbp) of TeO_4, with a small content of TeO_3 units with a terminal oxygen doubled bonded to the Te atom [79,81]. The structural units are highly asymmetric and have a large variation of bond length, due to the lone pair of electrons in one of the equatorial sites [79,82–85], which repel each other and also repel other oxygen atoms, strongly constraining the structure [86].

In their recent work, Hauke et al. [87] observed that the glass transition temperature of alkali tellurites tends to decrease monotonically with the increase of alkali content between 0 and 30 molar percent of R_2O. The addition of alkaline earth oxides, however, has the opposite effect, as T_g shows an increase with the RO content. The findings of the authors are in agreement with what we observed in this work (see supplementary materials). However, an establishment of a relation between structure and the observed trend in T_g of tellurites is challenging, mainly due to their structural complexity.

In 1992, Sekiya et al. [83] suggested that when alkali network modifiers are added to TeO_2, some $Te_{-eq}O_{ax-}Te$ (eq = equatorial and axe = axial sites) linkages are broken, and non-bridging-oxygens (NBO) are formed [79,83,88]. As a result, many more arrangements are possible, and we observed an increase in the glass stability, as shown in the ΔT_{rg} results (Fig. 4). However, the change is not monotonic, there is a maximum of GS around 20 molar percent of Li_2O and Na_2O (the two systems for which we have enough data), which agrees with the findings of Heo et al. [89] and McLaughlin et al. [90]. The explanation proposed by McLaughlin et al. [90] is that the intermediate range order of the 20% R_2O glass differs substantially from that of its isochemical crystal. While the $Na_2Te_4O_9$ crystals, for example, have four-membered Te-O bond rings, the glass shows a wide ring size distribution, where these small 4-membered rings are not major components. Therefore, it would require a considerable structural rearrangement for crystallization. The 5 molar percent of Cs_2O Te glass has only a slightly better GS than pure TeO_2, and it decreases back to the telluria GS value when the Cs_2O content reaches 15 molar percent. In fact, Mochida et al. [91] observed a narrower range of glass formation for Cs_2O tellurites than for other alkali tellurite compositions. They reported a range of ~3–11 molar percent of Cs_2O; meanwhile a Kalampounias and Boghosian [88] reported a 0–20 molar percent of Cs_2O. However, the structural differences between Cs_2O and other alkali tellurites at 15 molar percent of R_2O is not clear at this point.

In Fig. 4 (right), the CaO and SrO tellurites show a slight increase of GS compared to pure TeO_2, a value which remains almost constant in the region studied. The overall GS is lower than those of the alkali tellurites. data for the CaO-TeO_2 system shown in the plot was collected from the work of Chagraoui et al. [92] because our calcium tellurite samples crystallized during cooling. Since we could vitrify the SrO-TeO_2 samples, and the BaO tellurites visibly showed greater GS, the GS of the alkaline earth modifiers in TeO_2 appear to increase with increasing

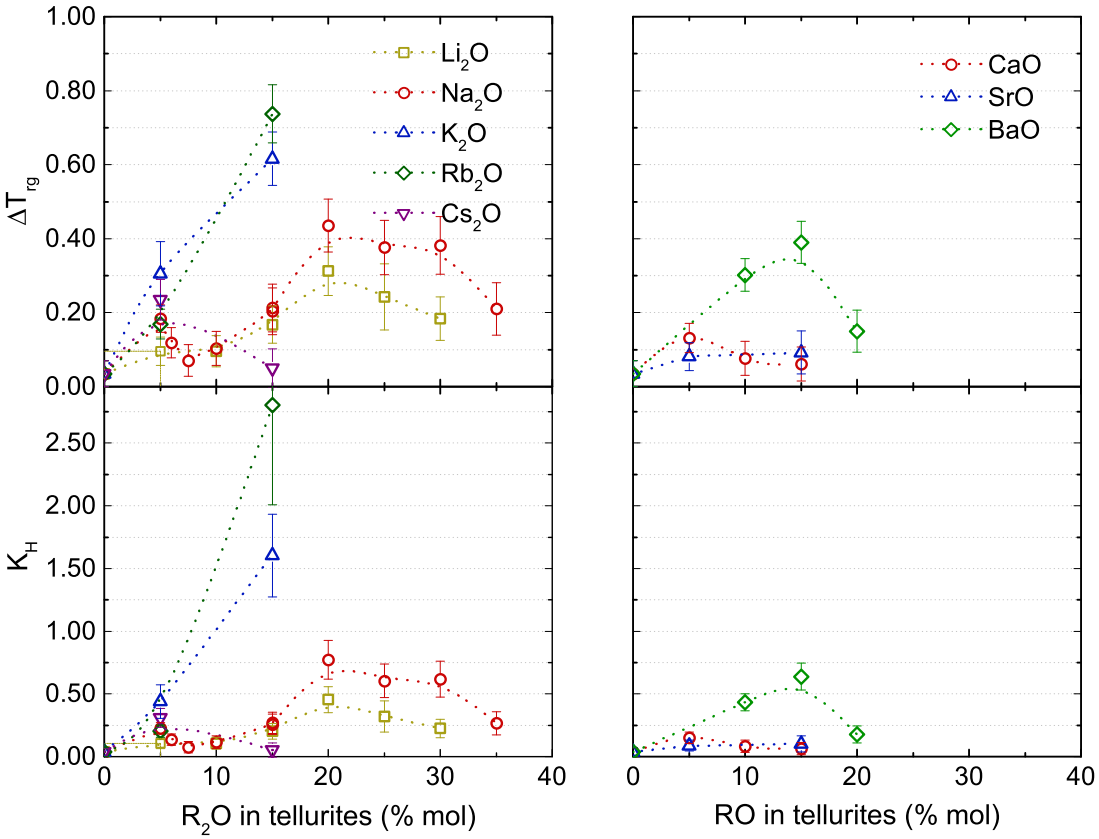

Fig. 4. Glass stability parameters ΔT_{rg} and K_H for a series of binary alkali (left) and alkaline earth (right) tellurite glasses. Powdered samples (particle size $<$ 100 μm), heating rate $=$ 20 K/minute.

cation radius. Data for the MgO-TeO_2 system is not available.

In the BaO-TeO_2 system the maximum GS occurs around 15 molar percent of BaO, different from what we found for the Li_2O and Na_2O tellurites. The effect of BaO on the structure of TeO_2 is very similar to that of the Li and Na effect. Between 5–20% of BaO, the glasses show a continuous network of TeO_4 trigonal bipyramids, TeO_{3+1} distorted trigonal bipyramids and TeO_3 trigonal pyramids. The greater the BaO content, the more TeO_4 units are converted to TeO_3 (by the formation of NBO's) [93].

The TeO_2 is the only system studied here that showed a noticeable different GS behavior of the alkaline earth modifiers. The liquidus temperatures of alkaline earth tellurites are very similar in the range studied, therefore, the structural differences between glass (or melt) and the nucleated crystal may play a more important role. However, the structural difference shown by the BaO-TeO_2 system in relation to other RO-TeO_2 is not clear enough to justify its better GS.

3.1.5. Aluminate glasses

Fig. 5 shows the glass stabilities of alkaline earth aluminates. Although liquid Al_2O_3 has a dominant proportion of AlO_4 tetrahedra, the Al-O coordination number and the presence of edge sharing polyhedra sharply increases with supercooling [94]. Pure alumina bulk glass has not been obtained via regular melt quenching. However, with addition of alkaline earth cations, the average coordination of Al-O decreases towards $n_{AlO} = 4$, and vitrification becomes possible.

The maximum values of ΔT_{rg} and $K_H \sim 0.20$–0.25 indicates a reluctant glass-former, low GS (and GFA), i.e., it is only possible to obtain small (mm thick samples) samples. The glass formation region of alkaline-earth aluminates has been explored before by Licheron and co-authors, and we have gotten similar results in our experiments in making these glasses by levitation. Attempts by other authors [95] and in this work to obtain magnesium aluminate glasses have failed. The CaO, SrO and BaO-Al_2O_3 standard glass formation region is approximately 45–75; 35–45/55–75 and 55–75 molar percent of RO, respectively. In the work of Kalamponias et al. [96] they reported calcium aluminates glasses with up to 80 molar percent of CaO using the same technique (ADL). Structural studies have pointed out that the connectivity of the glass network is reduced when the amount of RO is increased, and the influence of the cation radius is minor, i.e., there is no significant difference between the first order structures of CaO, SrO and BaO aluminates having equimolar percentages.

In fact, the glass stabilities of binary RO aluminates (Fig. 5 left) - alkaline-earth network modifiers - do not differ significantly. They are highest at around 65 molar percent of RO (the exact composition depends on the element), where deep eutectics occur. The maximum AlO_4 tetrahedral connectivity in the alkaline earth aluminate systems occurs at 50 molar percent of RO, which from a structural perspective, would reflect in greater GS and GFA, but the higher GS occurs in the eutectic. This implies that T_l is more important to the glass stability of these aluminates than the network connectivity of the glasses. The change in viscosity with temperature is more significant than with the increase of RO content, and the diffusion process required for crystallization are decelerated, hence it is expected that compositions with deep eutectics show better glass-forming ability and glass stability. The deep eutectic effect is also observed for the SiO_2 system, in compositions with more than 50 molar percent of modifier oxide.

3.2. Effect of the network modifiers on the GS

In Fig. 6, the ΔT_{rg} stability parameters of compositions containing Li, Na, Ca and Sr oxides are grouped by modifier type. Generally, as observed in the previous section, the larger the alkali modifier radius, the greater the glass stability. It is also seen that the ΔT_{rg} tends to be greater for the sodium glasses, reaching values as high as 0.5 for sodium

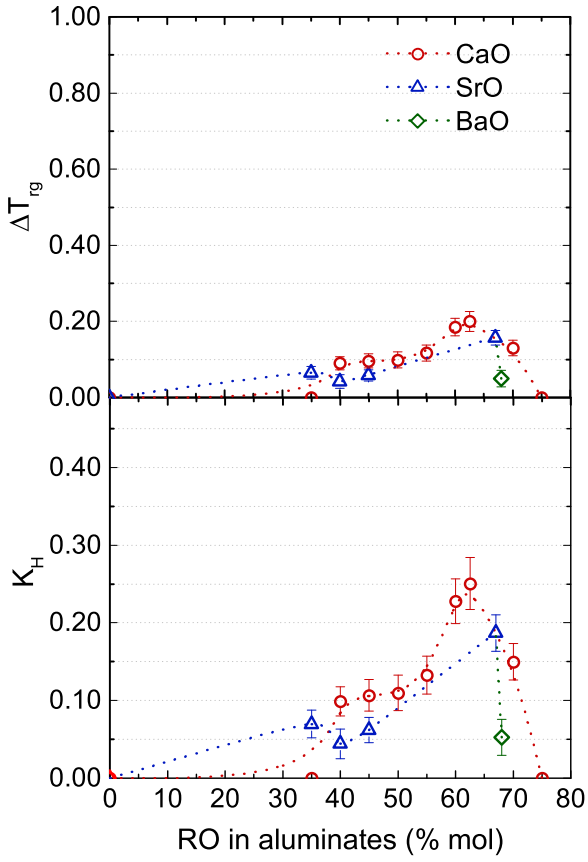

Fig. 5. Glass stability parameters ΔT_{rg} and K_H for a series of alkaline earth aluminate glasses. Powdered samples (particle size between 60 and 100 μm), heating rate = 20 K/minute.

silicates. For lithium-containing silicates, the maximum ΔT_{rg} is around 0.3. In the range of immiscibility - low lithium high SiO_2 content - for which there is no data, the GS could be higher, although it is not probable because of its high liquidus temperature. As observed in Section 3.1, for the good glass formers silica, boria and germania, the GS decreases with the increase of R_2O molar percent, and for the borates, the system we have plenty of data, a plateau is observed from 40 to 70 molar percent of R_2O. For the poor glass former telluria, the GS increases with the molar percent of R_2O and reaches a maximum at approximately 20 molar percent of R_2O. Differently from the alkalis, the alkaline earth elements have nearly the same effect in the GS of the glass formers studied, independent of their atomic radius. For the good glass formers, a sharp decrease of GS is observed for all alkaline earth ions, an effect similar to that of lithium, where all glasses have a ΔT_{rg} lower than 0.3. In alkaline earth silicates, for example, we can see the maxima at approximately 40 molar percent of RO, although the ΔT_{rg} is in the order of 0.2–0.3 (very low). The TeO_2 system is the only exception, for which BaO modified glasses show a higher GS. For the aluminates, the GS also increases with the addition of any modifier, and shows a maximum at 60–70 molar percent. The overall GS of silicate and borate glasses are the highest, without a distinction between them, followed by germanates, them by tellurites. The less stable glasses are the aluminates, hence the stability against crystallization decreases in the following order: $B > Si > Ge > Te > Al$. These findings revealed by the ΔT_{rg} parameter agree with our laboratory experience in making these glasses. However, some peculiarities about each system can change the relative order of GS proposed, for example, germanate and tellurite glasses have regions of minimum and maximum GS for the same amount of modifier. In this region, the tellurites are thermally more stable than the germanates.

Regarding the vitrificability, based on previous works [15,36,97] and some insights presented in the previous section (3.1), we could argue that the GS parameters are well related to the glass forming ability.

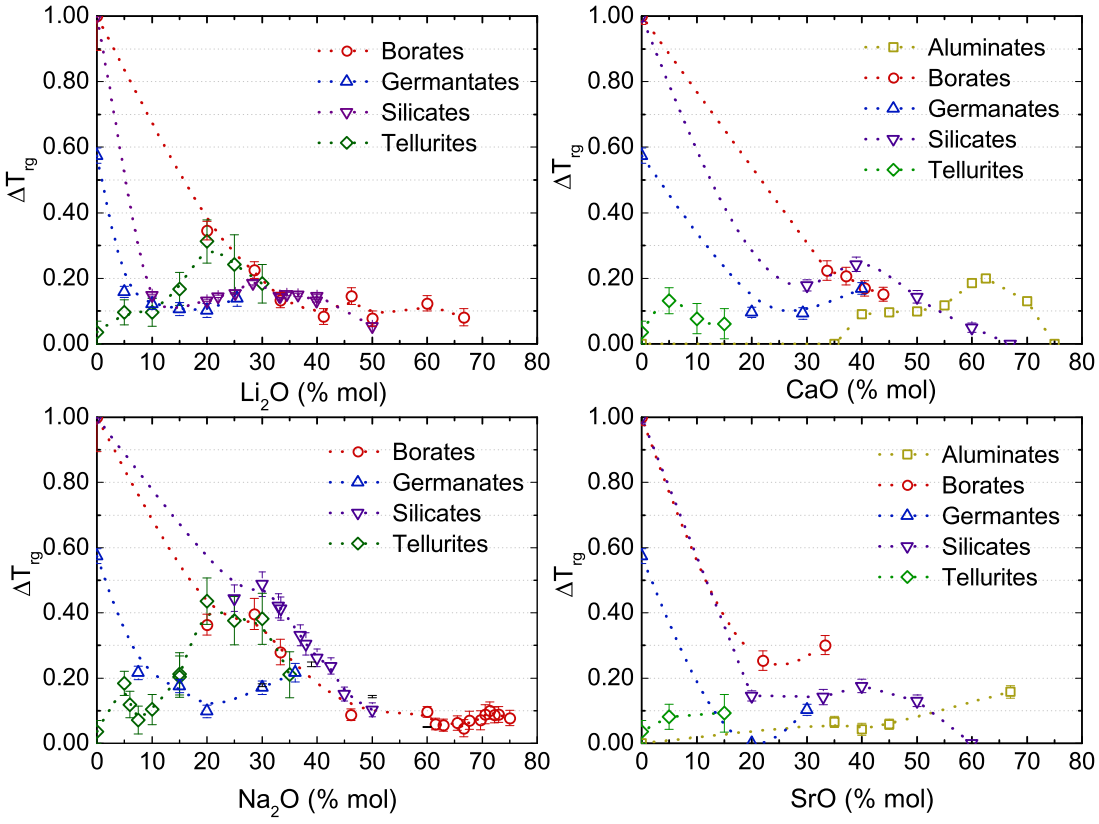

Fig. 6. ΔT_{rg} parameter for the alkali-modified glasses studied in this work. Left: lithium and sodium glasses. Right: calcium and strontium glasses.

In general, to improve the GS and GFA of glasses one has to increase the viscosity of the melt, which strongly depends of the network connectivity and temperature. Therefore, the content of network glass formers (SiO_2, B_2O_3 and GeO_2) has to be increased, and one should seek out for eutectic compositions, a fact that is already known empirically. A further increase of modifier content above 50% will have a minor influence on the viscosity of the liquid, thus, the presence of a deep eutectic is essential to achieve glass-formation by conventional methods in this region. The coordination number of the network former cations Ge, B, Al and Te change as the modifier content is increased and leads to specific behaviors in each system. The change in coordination can be beneficial to the GS, as in the cases of Al and Te, and can have a negative effect, as in the case of Ge. In the borates, we see no direct influence of the change of coordination in the GS with the data points we have available.

In the majority of systems, the substitution of Li by Na and K modifiers will increase GS and GFA. Between the alkaline earth modifiers, however, there is no difference in the effect, and when added individually to a glass former, the effect on the GS and GFA will be similar to Li. The tellurite system is the only system where the radius of the alkaline earth cation is important; for which the barium tellurites showed a better GS.

4. Conclusions

The two GS parameters used here indicate that for the good glass formers – silica, boria and germania – small additions of network *modifiers* rapidly reduce the GS and GFA. However, in the case of the conditional glass formers – telluria and alumina – the modifiers increase the GS and GFA. These findings are supported by empirical observations made during our laboratory glass melting practice. Regarding the effect of the alkalis, lithium containing glasses show the lowest GS, whereas glasses containing larger alkali cations are thermally more stable, however they are more hygroscopic. The alkaline earth modifiers have the same effect on the GS of most glass formers, except for TeO_2, for which the BaO tellurites show the best GS. For the majority of the studied systems, compositions having lower liquidus show better GS, especially for silicates and aluminates with modifier content above 50%, where the change in the viscosity by increasing modifier content is negligible.

As regards the network *glass-formers*, the pure oxides are ranked in the following sequence of GS: $B_2O_3 > SiO_2 > GeO_2 > TeO_2 > Al_2O_3$. However, structural peculiarities of each system sometimes change this order, as in the case of germanates and tellurites, which show the lowest and highest GS, respectively, for ~20 molar percent of modifier oxide.

Overall, the present findings give valuable insights for the design of novel crystallization resistant glasses.

CRediT authorship contribution statement

Jeanini Jiusti: Conceptualization, Methodology, Validation, Formal analysis, Investigation, Writing - review & editing, Visualization, Funding acquisition. **Edgar D. Zanotto:** Conceptualization, Resources, Supervision, Funding acquisition. **Steve A. Feller:** Resources, Supervision, Writing - review & editing. **Hayley J. Austin:** Methodology, Investigation. **Hanna M. Detar:** Methodology, Investigation. **Isabel Bishop:** Methodology, Investigation. **Danilo Manzani:** Methodology, Investigation, Writing - review & editing. **Yuko Nakatsuka:** Methodology, Investigation, Writing - review & editing. **Yasuhiro Watanabe:** Methodology, Investigation. **Hiroyuki Inoue:** Resources, Supervision, Writing - review & editing.

Declaration of Competing Interest

The authors declare that they have no known competing financial interests or personal relationships that could have appeared to influence the work reported in this paper.

Acknowledgements

We are thankful to the Brazilian agency São Paulo Research Foundation, FAPESP Project # 2013/007793–6 and Danilo's grant # 2018/16126–7, Jeanini´s grants CNPq # 141107/2016–2 and # 202646/2018–1. The NSF of the USA is thanked for support under grants NSF-DMR-1746230 and NSF-REU 1950337.

Supplementary materials

Supplementary material associated with this article can be found, in the online version, at doi:10.1016/j.jnoncrysol.2020.120359.

References

[1] J.E. Shelby, Thermal expansion of alkali borate glasses, J. Am. Ceram. Soc. 66 (1983) 225–227, https://doi.org/10.1111/j.1151-2916.1983.tb10023.x.
[2] J.E. Shelby, Effect of morphology on the properties of alkaline earth silicate glasses, J. Appl. Phys. 50 (1979) 8010–8015, https://doi.org/10.1063/1.325986.
[3] J.E. Shelby, J. Ruller, Properties and structure of lithium germanate glasses, Phys. Chem. Glas. Chemestry 28 (1987) 262–268.
[4] J.E. Shelby, Properties and structures of RO-GeO_2 glasses, J. Am. Ceram. Soc. 66 (1983) 414–416, https://doi.org/10.1111/j.1151-2916.1983.tb10072.x.
[5] J.E. Shelby, Viscosity and thermal expansion of alkali germanate glasses, J. Am. Ceram. Soc. 57 (1974) 436–439, https://doi.org/10.1111/j.1151-2916.1974.tb11376.x.
[6] D.R. Uhlmann, R.R. Shaw, The thermal expansion of alkali borate glasses and the boric oxide anomaly, J. Non. Cryst. Solids. 1 (1969) 347–359, https://doi.org/10.1016/0022-3093(69)90018-0.
[7] Y.D. Yiannopoulos, G.D. Chryssikos, E.I. Kamitsos, Structure and properties of alkaline earth borate glasses, Phys. Chem. Glas. 42 (2001) 164–172, https://doi.org/10.1098/rsif.2008.0348.
[8] J.M. Lewis, C.P. O'Brien, M. Affatigato, S.A. Feller, Physical properties of alkali and mixed lithium-cesium vanadate glasses prepared over an extended range of compositions, J. Non. Cryst. Solids. 293–295 (2001) 663–668, https://doi.org/10.1016/S0022-3093(01)00844-4.
[9] N.P. Lower, J.L. McRae, H.A. Feller, A.R. Betzen, S. Kapoor, M. Affatigato, S.A. Feller, Physical properties of alkaline-earth and alkali borate glasses prepared over an extended range of compositions, J. Non. Cryst. Solids. 293–295 (2001) 669–675, https://doi.org/10.1016/S0022-3093(01)00768-2.
[10] H.F. Shermer, Thermal expansion of binary alkaline-earth borate glasses, J. Res. Natl. Bur. Stand 56 (1956) (1934) 73, https://doi.org/10.6028/jres.056.010.
[11] J.M.F. Navarro, El vidrio, 3rd ed, Artegraf S.A, Madrid, Spain, 2003.
[12] A. Hrubý, Evaluation of glass-forming tendency by means of DTA, Czechoslov. J. Phys 22 (1972) 1187–1193, https://doi.org/10.1007/BF01690134.
[13] D.R. Uhlmann, A kinect treatment of glass formation, J. Non. Cryst. Solids. 7 (1972) 337–348, https://doi.org/10.1016/0022-3093(72)90269-4.
[14] M.C. Weinberg, Glass-forming ability and glass stability in simple systems, J. Non. Cryst. Solids. 167 (1994) 81–88, https://doi.org/10.1016/0022-3093(94)90370-0.
[15] A.A. Cabral, A.A.D. Cardoso, E.D. Zanotto, Glass-forming ability versus stability of silicate glasses. I. Experimental test, J. Non. Cryst. Solids. 320 (2003) 1–8, https://doi.org/10.1016/S0022-3093(03)00079-6.
[16] J. Jiusti, D.R. Cassar, E.D. Zanotto, Which glass stability parameters can assess the glassforming ability of oxide systems? Int. J. Appl. Glas. Sci. (2020), https://doi.org/10.1111/ijag.15416 online ver.
[17] D.R. Uhlmann, H. Yinnon, The formation of glasses, in: D.R Uhlmann, N.J. Kreidl (Eds.), Glas. Technol. Academic Press, New York, 1983, pp. 1–47.
[18] E. Asayama, H. Takebe, K. Morinaga, Critical cooling rates for the formation of glass for silicate melts, ISIJ Int 33 (1993) 233–238, https://doi.org/10.2355/isijinternational.33.233.
[19] J.M. Barandiarán, J. Colmenero, Continuous cooling approximation for the formation of a glass, J. Non. Cryst. Solids. 46 (1981) 277–287, https://doi.org/10.1016/0022-3093(81)90006-5.
[20] Q. Chen, J. Shen, D. Zhang, H. Fan, J. Sun, D.G. McCartney, A new criterion for evaluating the glass-forming ability of bulk metallic glasses, Mater. Sci. Eng. A. 433 (2006) 155–160, https://doi.org/10.1016/j.msea.2006.06.053.
[21] G.J. Fan, H. Choo, P.K. Liaw, A new criterion for the glass-forming ability of liquids, J. Non. Cryst. Solids. 353 (2007) 102–107, https://doi.org/10.1016/j.jnoncrysol.2006.08.049.
[22] X.H. Du, J.C. Huang, C.T. Liu, Z.P. Lu, New criterion of glass forming ability for bulk

metallic glasses, J. Appl. Phys. 101 (2007) 1–4, https://doi.org/10.1063/1.2718286.
[23] X.H. Du, J.C. Huang, New criterion in predicting glass forming ability of various glass-forming systems ability, Chinese Phys. B. 17 (2008) 249.
[24] Z.Z. Yuan, S.L. Bao, Y. Lu, D.P. Zhang, L. Yao, A new criterion for evaluating the glass-forming ability of bulk glass forming alloys, J. Alloys Compd 459 (2008) 251–260, https://doi.org/10.1016/j.jallcom.2007.05.037.
[25] Z. Long, H. Wei, Y. Ding, P. Zhang, G. Xie, A. Inoue, A new criterion for predicting the glass-forming ability of bulk metallic glasses, J. Alloys Compd 475 (2009) 207–219, https://doi.org/10.1016/j.jallcom.2008.07.087.
[26] Z. Long, G. Xie, H. Wei, X. Su, J. Peng, P. Zhang, A. Inoue, On the new criterion to assess the glass-forming ability of metallic alloys, Mater. Sci. Eng. A. 509 (2009) 23–30, https://doi.org/10.1016/j.msea.2009.01.063.
[27] P. Zhang, H. Wei, X. Wei, Z. Long, X. Su, Evaluation of glass-forming ability for bulk metallic glasses based on characteristic temperatures, J. Non. Cryst. Solids. 355 (2009) 2183–2189, https://doi.org/10.1016/j.jnoncrysol.2009.06.001.
[28] X. Ji, Y. Pan, A thermodynamic approach to assess glass-forming ability of bulk metallic glasses, Trans. Nonferrous Met. Soc (2009) 1271–1279, https://doi.org/10.1016/S1003-6326(08)60438-0 China (English Ed. 19.
[29] G.H. Zhang, K.C. Chou, A criterion for evaluating glass-forming ability of alloys, J. Appl. Phys (2009) 106, https://doi.org/10.1063/1.3255952.
[30] D. Turnbull, Under what conditions can a glass be formed? Contemp. Phys. 10 (1969) 473–488, https://doi.org/10.1080/00107516908204405.
[31] S. Guo, C.T. Liu, New glass forming ability criterion derived from cooling consideration, Intermetallics 18 (2010) 2065–2068, https://doi.org/10.1016/j.intermet.2010.06.012.
[32] B.S. Dong, S.X. Zhou, D.R. Li, C.W. Lu, F. Guo, X.J. Ni, Z.C. Lu, A new criterion for predicting glass forming ability of bulk metallic glasses and some critical discussions, Prog. Nat. Sci. Mater. Int. 21 (2011) 164–172, https://doi.org/10.1016/S1002-0071(12)60051-3.
[33] I.G. Polyakova, Structure of glass near eutectics of phase diagrams on the example of the barium-borate system according to the DTA data, Glas. Phys. Chem. 41 (2015) 48–53, https://doi.org/10.1134/S1087659615010216.
[34] M.K. Tripathi, P.P. Chattopadhyay, S. Ganguly, A predictable glass forming ability expression by statistical learning and evolutionary intelligence, Intermetallics 90 (2017) 9–15, https://doi.org/10.1016/j.intermet.2017.06.008.
[35] A.M. Rodrigues, L.D. Silva, R. Zhang, V.O. Soares, Structural effects on glass stability and crystallization, CrystEngComm (2018) 2–7, https://doi.org/10.1039/C7CE02135F.
[36] M.L.F. Nascimento, L.A. Souza, E.B. Ferreira, E.D. Zanotto, Can glass stability parameters infer glass forming ability? J. Non. Cryst. Solids 351 (2005) 3296–3308, https://doi.org/10.1016/j.jnoncrysol.2005.08.013.
[37] A. Inoue, T. Zhang, T. Masumoto, Glass-forming ability of alloys, J. Non. Cryst. Solids. 158 (1993) 49–144, https://doi.org/10.1201/9781420085976-1.
[38] M. Saad, M. Poulain, Glass-forming ability criterion, Mater. Sci. Forum 19–20 (1987) 11–18, https://doi.org/10.4028/www.scientific.net/MSF.19-20.11.
[39] T. Wakasugi, R. Ota, J. Fukunaga, Glass-forming ability and crystallization tendency evaluated by the DTA method in the Na_2O–B_2O_3–Al_2O_3 system, J. Am. Ceram. Soc. 75 (1992) 3129–3132, https://doi.org/10.1111/j.1151-2916.1992.tb04398.x.
[40] Z.P. Lu, C.T. Liu, A new glass-forming ability criterion for bulk metallic glasses, Acta Mater 50 (2002) 3501–3512, https://doi.org/10.1016/S1359-6454(02)00166-0.
[41] Y. Zhang, D.Q. Zhao, M.X. Pan, W.H. Wang, Relationship between glass forming ability and thermal parameters of Zr based bulk metallic glasses, Mater. Sci. Technol. 19 (2003) 973–976, https://doi.org/10.1179/026708303225003045.
[42] K. Mondal, B.S. Murty, On the parameters to assess the glass forming ability of liquids, J. Non. Cryst. Solids. 351 (2005) 1366–1371, https://doi.org/10.1016/j.jnoncrysol.2005.03.006.
[43] A.A. Cabral, C. Fredericci, E.D. Zanotto, A test of the Hrubÿ parameter to estimate glass-forming ability, J, Non. Cryst. Solids. 219 (1997) 182–186, https://doi.org/10.1016/S0022-3093(97)00327-X.
[44] A.F. Kozmidis-Petrović, Theoretical analysis of relative changes of the Hruby, Weinberg, and Lu-Liu glass stability parameters with application on some oxide and chalcogenide glasses, Thermochim. Acta 499 (2010) 54–60, https://doi.org/10.1016/j.tca.2009.10.023.
[45] A. Kozmidis-Petrovic, J. Šesták, Forty years of the Hrubý glass-forming coefficient via DTA when comparing other criteria in relation to the glass stability and vitrification ability, J. Therm. Anal. Calorim. 110 (2012) 997–1004, https://doi.org/10.1007/s10973-011-1926-6.
[46] E.B. Ferreira, E.D. Zanotto, S. Feller, G. Lodden, J. Banerjee, T. Edwards, M. Affatigato, Critical analysis of glass stability parameters and application to lithium borate glasses, J. Am. Ceram. Soc. 94 (2011) 3833–3841, https://doi.org/10.1111/j.1551-2916.2011.04767.x.
[47] A.J. Havel, S.A. Feller, M. Affatigato, M. Karns, Design and operation of a new roller quencher for rapidly cooling melts into glasses, Glas. Technol. Eur. J. Glas. Sci. Technol 50 (2009) 227–229 Part A..
[48] C.J. Benmore, J.K.R. Weber, Aerodynamic levitation, supercooled liquids and glass formation, Adv. Phys. X. 2 (2017) 717–736, https://doi.org/10.1080/23746149.2017.1357498.
[49] D.H. Kang, H. Zhang, H. Yoo, H.H. Lee, S. Lee, G.W. Lee, H. Lou, X. Wang, Q. Cao, D. Zhang, J. Jiang, Interfacial free energy controlling glass-forming ability of Cu-Zr alloys, Sci. Rep. 4 (2014) 1–5, https://doi.org/10.1038/srep05167.
[50] J. Russo, F. Romano, H. Tanaka, Glass forming ability in systems with competing orderings, Phys. Rev. X 8 (2018) 21040, https://doi.org/10.1103/PhysRevX.8.021040.
[51] E.D. Zanotto, J.E. Tsuchida, J.F. Schneider, H. Eckert, Thirty-year quest for structure-nucleation relationships in oxide glasses, Int. Mater. Rev. 60 (2015) 376–391, https://doi.org/10.1080/09506608.2015.1114706.
[52] P.I.K. Onorato, D.R. Uhlmann, Nucleating heterogeneities and glass formation, J. Non. Cryst. Solids 22 (1976) 367–378, https://doi.org/10.1016/0022-3093(76)90066-1.
[53] J. Jiusti, E.D. Zanotto, D.R. Cassar, M.R.B. Andreeta, Viscosity and liquidus-based predictor of glass-forming ability of oxide glasses, J. Am. Ceram. Soc. 103 (2020) 921–932, https://doi.org/10.1111/jace.16732.
[54] B.E. Warren, J. Biscce, The structure of silica glass by X-ray diffraction studies, J. Am. Ceram. Soc. 21 (1938) 49–54, https://doi.org/10.1111/j.1151-2916.1938.tb15742.x.
[55] R.J. Charles, Metastable liquid immiscibility in alkali metal oxide–silica systems, J. Am. Ceram. Soc. 49 (1966) 55–62, https://doi.org/10.1111/j.1151-2916.1966.tb13208.x.
[56] P. Hudon, D.R. Baker, The nature of phase separation in binary oxide melts and glasses part 3: borate and germanate systems, J. Non. Cryst. Solids. 303 (2002) 354–371, https://doi.org/10.1002/chin.200235258.
[57] C. Larson, J. Doerr, M. Affatigato, S. Feller, D. Holland, M.E. Smith, A ^{29}Si MAS NMR study of silicate glasses with a high lithium content, J. Phys. Condens. Matter. 18 (2006) 11323–11331, https://doi.org/10.1088/0953-8984/18/49/023.
[58] R. Dupree, D. Holland, D.S. Williams, The structure of binary alkali silicate glasses, J. Non. Cryst. Solids. 81 (1986) 185–200.
[59] V.N. Bykov, A.A. Osipov, V.N. Anfilogov, Structural study of rubidium and caesium silicate glasses by Raman spectroscopy, Phys. Chem. Glas 41 (2000) 10–11.
[60] J.G. Longstaffe, U. Werner-Zwanziger, J.F. Schneider, M.L.F. Nascimento, E.D. Zanotto, J.W. Zwanziger, Intermediate-range order of alkali disilicate glasses and its relation to the devitrification mechanism, J. Phys. Chem. C. 112 (2008) 6151–6159, https://doi.org/10.1021/jp711438v.
[61] A. Einstein, On the movement of small particles suspended in stationary liquids required by the molecular-kinetic theory of heat, Ann. Phys. 17 (1905) 549–560, https://doi.org/10.1002/andp.19053220806.
[62] H. Eyring, plasticity Viscosity, and diffusion as examples of absolute reaction rates, J. Chem. Phys. 4 (1936) 283–291, https://doi.org/10.1063/1.1749836.
[63] E.D. Zanotto, D.R. Cassar, The microscopic origin of the extreme glass-forming ability of Albite and B_2O_3, Sci. Rep. 7 (2017) 43022, https://doi.org/10.1038/srep43022.
[64] R.R. Shaw, D.R. Uhlmann, Subliquidus immiscibility in binary alkali borates, J. Am. Ceram. Soc. 51 (1968) 377–382, https://doi.org/10.1111/j.1151-2916.1968.tb11897.x.
[65] H. Yu, Q. Chen, Z. Jin, Thermodynamic assessment of the CaO-B_2O_3 system, Calphad Comput. Coupling Phase Diagrams Thermochem 23 (1999) 101–111, https://doi.org/10.1016/S0364-5916(99)00016-4.
[66] H. Yu, Q. Chen, Thermodynamic reassessment of the BaO-B_2O_3 system, J. Phase Equilibria 20 (1999) 479–484, https://doi.org/10.1361/105497199770340734.
[67] X.M. Pan, C.P. Wang, Z. Jin, Assessment of the thermodynamics and phase diagram of the SrO-B_2O_3 system, Zeitschrift Für Met 95 (2004) 40–44, https://doi.org/10.3139/146.017908.
[68] S. Miyagawa, S. Hirano, S. Somiya, Phase relations in the system MgO-B_2O_3 and effects of boric oxide on grain growth of magnesia, Yogyo Kyokaishi 80 (1972) 53–63.
[69] L. Cormier, O. Majérus, D.R. Neuville, G. Calas, Temperature-induced structural modifications between alkali borate glasses and melts, J. Am. Ceram. Soc. 89 (2006) 13–19, https://doi.org/10.1111/j.1551-2916.2005.00657.x.
[70] M. Micoulaut, L. Cormier, G.S. Henderson, The structure of amorphous, crystalline and liquid GeO_2, J. Phys. Condens. Matter. 18 (2006), https://doi.org/10.1088/0953-8984/18/45/R01.
[71] J.A.E. Desa, A.C. Wright, R.N. Sinclair, A neutron diffraction investigation of the structure of vitreous germania, J. Non. Cryst. Solids. 99 (1988) 276–288, https://doi.org/10.1016/0022-3093(88)90437-1.
[72] J.C.A. Vreeswijk, R.G. Gossink, J.M. Stevels, Nucleation kinetics and critical cooling rate of glass-forming liquids, J. Non. Cryst. Solids. 16 (1974) 15–26, https://doi.org/10.1016/0022-3093(74)90065-9.
[73] S. Sakaguchi, Evaluation of the critical cooling rate in glass-forming materials based on viscosity, J. Non. Cryst. Solids. 185 (1995) 268–273, https://doi.org/10.1016/0022-3093(94)00682-2.
[74] Y. Tabata, Y. Ohta, K. ji Morinaga, T. Yanagase, Immiscible region in binary germanate systems, Yogyo Kyokai Shi/Journal Ceram. Soc. Japan 91 (1983) 509–516, https://doi.org/10.2109/jcersj1950.91.1059_509.
[75] R.R. Shaw, D.R. Uhlmann, Effect of phase separation on the properties of simple glasses I. Density and molar volume, J. Non. Cryst. Solids. 1 (1969) 474–498, https://doi.org/10.1016/0022-3093(69)90009-X.
[76] J.E. Shelby, Introduction to glass science and technology, 1999. 10.1524/zpch.1999.208.Part_1_2.292.
[77] G.S. Henderson, The germanate anomaly: what do we know? J. Non. Cryst. Solids. 353 (2007) 1695–1704, https://doi.org/10.1016/j.jnoncrysol.2007.02.037.
[78] O.L.G. Alderman, A.C. Hannon, S. Feller, R. Beanland, D. Holland, The germanate anomaly in alkaline earth germanate glasses, J. Phys. Chem. C. 121 (2017) 9462–9479, https://doi.org/10.1021/acs.jpcc.6b12372.
[79] E.R. Barney, A.C. Hannon, D. Holland, N. Umesaki, M. Tatsumisago, R.G. Orman, S. Feller, Terminal oxygens in amorphous TeO_2, J. Phys. Chem. Lett. 4 (2013) 2312–2316, https://doi.org/10.1021/jz4010637.
[80] N.S. Tagiara, D. Palles, E.D. Simandiras, V. Psycharis, A. Kyritsis, E.I. Kamitsos, Synthesis, thermal and structural properties of pure TeO_2 glass and zinc-tellurite glasses, J. Non. Cryst. Solids. 457 (2017) 116–125, https://doi.org/10.1016/j.jnoncrysol.2016.11.033.
[81] M.A.T. Marple, M. Jesuit, I. Hung, Z. Gan, S. Feller, S. Sen, Structure of TeO_2 glass:

results from 2D ^{125}Te NMR spectroscopy, J. Non. Cryst. Solids. 513 (2019) 183–190, https://doi.org/10.1016/j.jnoncrysol.2019.03.019.
[82] O. Lindqvist, Refinement of the structure of α-TeO_2, Acta Chem. Scand. 22 (1968) 977–982.
[83] T. Sekiya, N. Mochida, A. Ohtsuka, M. Tonokawa, Raman spectra of $MO_{1/2}$-TeO_2 (M=Li, Na, K, Rb, Cs an Tl) glasses, J. Non. Cryst. Solids. 144 (1992) 128–144, https://doi.org/10.1016/S0022-3093(05)80393-X.
[84] M.N. Garaga, U. Werner-Zwanziger, J.W. Zwanziger, A. Deceanne, B. Hauke, K. Bozer, S. Feller, Short-range structure of TeO_2 glass, J. Phys. Chem. C. 121 (2017) 28117–28124, https://doi.org/10.1021/acs.jpcc.7b08978.
[85] O.L.G. Alderman, C.J. Benmore, S. Feller, E.I. Kamitsos, E.D. Simandiras, D.G. Liakos, M. Jesuit, M. Boyd, M. Packard, R. Weber, Short-range disorder in TeO_2 melt and glass, J, Phys. Chem. Lett. 11 (2020) 427–431, https://doi.org/10.1021/acs.jpclett.9b03231.
[86] R.A. Narayanan, J.W. Zwanziger, The glass forming ability of tellurites: a rigid polytope approach, J. Non. Cryst. Solids. 316 (2003) 273–280, https://doi.org/10.1016/S0022-3093(02)01598-3.
[87] B. Hauke, E.R. Barney, E. Pakhomenko, M. Jesuit, M. Packard, A. Crego, G. Tarantino, M. Affatigato, S. Feller, Structure and glass transition temperatures of tellurite glasses, Phys. Chem. Glas. Eur. J. Glas. Sci. Technol. (2020) 21–26, https://doi.org/10.13036/17533562.61.1.11 Part B. 61.
[88] A.G. Kalampounias, S. Boghosian, Distribution of tellurite polymorphs in the xM_2O-(1 - X)TeO_2(M = Li, Na, K, Cs, and Rb) binary glasses using Raman spectroscopy, Vib. Spectrosc 59 (2012) 18–22, https://doi.org/10.1016/j.vibspec.2011.12.013.
[89] J. Heo, D. Lam, G.H. Sigel, E.A. Mendoza, D.A. Hensley, Spectroscopic analysis of the structure and properties of alkali tellurite glasses, J. Am. Ceram. Soc. 75 (1992) 277–281, https://doi.org/10.1111/j.1151-2916.1992.tb08176.x.
[90] J.C. McLaughlin, S.L. Tagg, J.W. Zwanziger, D.R. Haeffner, S.D. Shastri, Structure of tellurite glass: a combined NMR, neutron diffraction, and X-ray diffraction study, J. Non. Cryst. Solids. 274 (2000) 1–8, https://doi.org/10.1016/S0022-3093(00)00199-X.
[91] N. Mochida, K. Takahashi, K. Nakata, S. Shibusawa, Properties and containing structure of the binary tellurite cations glasses containing mono- and di-valent cations, Yogyo Kyokai Shi 86 (1978) 316–326, https://doi.org/10.2109/jcersj1950.86.995_316.
[92] A. Chagraoui, A. Tairi, K. Ajebli, H. Bensaid, A. Moussaoui, New tellurite glasses and crystalline phases in the Bi_2O_3-CaO-TeO_2 system: synthesis and characterization, J. Alloys Compd. 495 (2010) 67–71, https://doi.org/10.1016/j.jallcom.2009.11.115.
[93] T. Sekiya, N. Mochida, A. Ohtsuka, Raman spectra of $MOTeO_2$(M = Mg, Sr, Ba and Zn) glasses, J. Non. Cryst. Solids. 168 (1994) 106–114, https://doi.org/10.1016/0022-3093(94)90125-2.
[94] C. Shi, O.L.G. Alderman, D. Berman, J. Du, J. Neuefeind, A. Tamalonis, J.K.R. Weber, J. You, C.J. Benmore, The structure of amorphous and deeply supercooled liquid alumina, Front. Mater 6 (2019) 1–15, https://doi.org/10.3389/fmats.2019.00038.
[95] M. Licheron, V. Montouillout, F. Millot, D.R. Neuville, Raman and ^{27}Al NMR structure investigations of aluminate glasses: (1 - x)Al_2O_3 - x MO, with M = Ca, Sr, Ba and 0.5, J. Non. Cryst. Solids. 357 (2011) 2796–2801, https://doi.org/10.1016/j.jnoncrysol.2011.03.001.
[96] A.G. Kalampounias, N. Nasikas, Y. Pontikes, G.N. Papatheodorou, Thermal properties of calcium aluminate xCaO-(1-x)Al_2O_3 glasses, Phys. Chem. Glas. 53 (2012) 205–209, https://doi.org/10.4191/kcers.2010.47.2.117.
[97] T.V.R. Marques, A.A. Cabral, Influence of the heating rates on the correlation between glass-forming ability (GFA) and glass stability (GS) parameters, J. Non. Cryst. Solids. 390 (2014) 70–76, https://doi.org/10.1016/j.jnoncrysol.2014.02.019.